

Vegard's law

A. R. Denton and N. W. Ashcroft

Laboratory of Atomic and Solid State Physics and Materials Science Center, Cornell University, Ithaca, New York 14853-2501

(Received 26 November 1990)

Vegard's law is an approximate empirical rule which holds that a *linear* relation exists, at constant temperature, between the crystal lattice constant of an alloy and the concentrations of the constituent elements. Applications of a density-functional theory of nonuniform fluid mixtures to the fluid-solid transition of simple binary mixtures of hard spheres demonstrates the importance of relative atomic sizes in determining lattice constants and suggests that for sufficiently small disparities in atomic size Vegard's law may also hold along the fluid-solid coexistence curve.

A fundamental problem in the theory and practice of alloy formation is the manner in which the microscopic crystal structures of alloys (solid mixtures) depend on the atomic properties and relative concentrations of the constituent elements. In an early application of x-ray diffraction to the analysis of crystal structure, Vegard¹ observed that in many ionic salt alloys a *linear* relation held, at constant temperature, between the crystal lattice constant and concentration. This empirical rule has since come to be known as "Vegard's law," although in subsequent extensions of the rule to metallic alloys the majority of systems have been found not to obey it.²⁻⁴

Several physical factors affecting the crystal structures assumed by alloys can be readily identified.⁵ These include (i) the relative atomic sizes of the elements, (ii) the relative volume per valence electron in crystals of the pure elements, (iii) Brillouin-zone effects, and (iv) electrochemical differences between the elements. Here, we examine the role of the atomic-size factor alone by considering an idealized model mixture of hard spheres. This is not to deny the importance of the other factors, but rather to demonstrate that the simple but intuitively important geometric factor of differing atomic sizes, by itself, can play a significant role in determining the crystal structures of alloys. Our approach is based on a density-functional theory of classical nonuniform fluid mixtures, which we recently proposed and also applied to fluid-solid transitions in binary mixtures of hard spheres.^{6,7} We report here an important additional outcome of this application, namely a prediction for the concentration dependence of the lattice constant of a random binary hard-sphere alloy under coexistence conditions with the fluid. By varying the ratio of the hard-sphere diameters, we are able to study the form of the lattice-constant-concentration relationship as a function of the disparity in atomic sizes between the two components and relate the results of Vegard's law. We note that the relationship between density-functional theory and Vegard's law has been briefly discussed by Barrat, Baus, and Hansen.⁸

The central quantity in our density-functional theory⁶ is the (Helmholtz) free energy $F[\rho_1, \rho_2]$, a unique functional of the two spatially varying densities, $\rho_1(\mathbf{r})$ and $\rho_2(\mathbf{r})$, which is minimized at constant average density by

the equilibrium densities.⁹ It is useful to separate $F[\rho_1, \rho_2]$ into physically distinct contributions by writing

$$F[\rho_1, \rho_2] = F_{\text{id}}[\rho_1, \rho_2] + F_{\text{ex}}[\rho_1, \rho_2], \quad (1)$$

where F_{id} is the *ideal-gas* free energy of the nonuniform system in the absence of interactions and F_{ex} is the *excess* free energy, originating in internal interactions. (We assume here the absence of any external potential.) The advantage of this separation is that F_{id} may be expressed exactly in the form

$$\beta F_{\text{id}}[\rho_1, \rho_2] = \sum_{i=1}^2 \int d\mathbf{r} \rho_i(\mathbf{r}) \{ \ln[\rho_i(\mathbf{r}) \lambda_i^3] - 1 \}, \quad (2)$$

where $\beta \equiv 1/k_B T$ and λ_i denotes the thermal de Broglie wavelength of component i . In contrast, the exact F_{ex} is unknown and is here approximated by a straightforward generalization to mixtures⁶ of the modified weighted-density approximation¹⁰ (MWDA). In its original formulation for one-component systems, the MWDA is based on the assumption that F_{ex} for a nonuniform fluid may be equated to its uniform-fluid counterpart, which is evaluated, however, at an *effective* density defined as a certain *weighted average* of the physical density (see Ref. 10 for details). Our generalization to binary mixtures is expressed by setting

$$F_{\text{ex}}^{\text{MWDA}}[\rho_1, \rho_2]/N \equiv (1-x)f_0(\hat{\rho}^{(1)}, x) + xf_0(\hat{\rho}^{(2)}, x), \quad (3)$$

where N is the number of particles, x is the average concentration (of component 2, by convention) in the nonuniform mixture, f_0 is the excess free energy per particle of the *uniform* mixture, and where $\hat{\rho}^{(1)}$ and $\hat{\rho}^{(2)}$ denote *total* "weighted densities." The latter are defined as bilinear weighted averages of the physical densities with respect to weight functions \bar{w}_{ij} according to

$$\hat{\rho}^{(i)} \equiv \frac{1}{N_i} \sum_{j=1}^2 \int d\mathbf{r} \int d\mathbf{r}' \rho_i(\mathbf{r}) \rho_j(\mathbf{r}') \bar{w}_{ij}(|\mathbf{r} - \mathbf{r}'|; \hat{\rho}^{(i)}), \quad i = 1, 2, \quad (4)$$

where N_i is the number of particles of component i . As in the one-component case, the self-consistent choice of the density argument of \bar{w}_{ij} in Eq. (4) is essential.⁶ To en-

sure that the approximation is exact in the uniform limit $[\rho(\mathbf{r}) \rightarrow \rho_0]$, the \bar{w}_{ij} must be normalized according to

$$\int d\mathbf{r}' \bar{w}_{ij}(|\mathbf{r}-\mathbf{r}'|) = 1, \quad i, j = 1, 2. \quad (5)$$

A unique specification of the weight functions \bar{w}_{ij} follows from requiring that $F_{\text{ex}}^{\text{MWDA}}$ exactly satisfies the defining relations

$$-\beta \lim_{\rho(\mathbf{r}) \rightarrow \rho_0} \left[\frac{\delta^2 F_{\text{ex}}[\rho_1, \rho_2]}{\delta \rho_i(\mathbf{r}) \delta \rho_j(\mathbf{r}')} \right] = c_{ij}^{(2)}(|\mathbf{r}-\mathbf{r}'|), \quad i, j = 1, 2 \quad (6)$$

for $c_{ij}^{(2)}$, the two-particle (Ornstein-Zernike) direct correlation functions (DCF's) of the uniform mixture. Indeed, substitution of $F_{\text{ex}}^{\text{MWDA}}$ [Eq. (3)] into Eq. (6) yields simple analytic expressions for \bar{w}_{ij} involving the uniform-state functions f_0 and $c_{ij}^{(2)}$ (see Ref. 6). We note that specification of the weight functions according to Eqs. (5) and (6) ensures that the MWDA exactly satisfies two important sets of relations, namely the compressibility relations¹¹ and the hierarchy relations between $c_{ij}^{(2)}$ and higher-order DCF's.

Together, Eqs. (3)–(6) constitute our generalization of the MWDA to binary mixtures. Application to the fluid-solid (freezing) transition now involves three principal steps: (i) parametrization of the solid density, (ii) minimization of the total free energy with respect to this

parametrized density, and (iii) location of the transition at fluid-solid coexistence. Parametrization of the solid density requires both the choice of a crystal structure and an assumption for the form of the density distribution about the lattice sites of the chosen crystal. Here we assume, by way of example, a disordered-fcc structure, taking the atoms of the two components to be distributed *randomly* over the sites of a perfect fcc lattice, and a simple Gaussian distribution of the form

$$\rho_i(\mathbf{r}) = x_i \left[\frac{\gamma_i}{\pi} \right]^{3/2} \sum_{\mathbf{R}} \exp^{-\gamma_i |\mathbf{r}-\mathbf{R}|^2}, \quad i = 1, 2, \quad (7)$$

where x_i is the concentration of component i , and γ_1 and γ_2 are “localization parameters” determining the widths of the Gaussians centered on the lattice sites at positions \mathbf{R} . It is important to note that the assumption of a random distribution of atoms on a perfect lattice ignores short-range order and local lattice distortions. Furthermore, the Gaussian approximation, although well tested in the one-component hard-sphere system both by simulation¹² and by comparison with alternative parametrizations,^{13–15} is still relatively untested in its application to mixtures. However, we expect it to be quite reasonable when the hard-sphere diameters of the two components are sufficiently similar, which is the case here.¹⁵

From Eqs. (4) and (7), the weighted densities can now be expressed as Fourier-space sums over the reciprocal-lattice vectors \mathbf{G} of the solid, according to

$$\hat{\rho}^{(i)}(\rho_s, x) = \rho_s \left\{ 1 - \frac{1}{2\beta f_0'(\hat{\rho}^{(i)}, x)} \sum_{j=1}^2 x_j \sum_{\mathbf{G} \neq 0} \exp \left[\frac{-G^2}{4} \left(\frac{1}{\gamma_i} + \frac{1}{\gamma_j} \right) \right] c_{ij}^{(2)}(\mathbf{G}; \hat{\rho}^{(i)}, x) \right\}, \quad (8)$$

where ρ_s is the average solid density, and the prime on f_0 signifies a partial derivative with respect to density. Equation (8) is a self-consistent relation for $\hat{\rho}^{(i)}$, which is easily solved—at fixed ρ_s , x , and γ_i —by numerical iteration.¹⁶ For the required uniform-state functions f_0 and $c_{ij}^{(2)}$, we adopt the expressions following from Lebowitz's analytic solution¹⁷ of the Percus-Yevick (PY) integral equation for hard-sphere mixtures. It is important to observe that in the MWDA these functions are always evaluated at weighted densities, and these are usually sufficiently low that the known high-density inaccuracies of the PY approximation¹⁸ are not expected to be significant. Substitution of $\hat{\rho}_i$ [Eq. (8)] into Eq. (3) now immediately gives $F_{\text{ex}}^{\text{MWDA}}$, and addition of F_{id} then yields the approximate total free energy F^{MWDA} . In the case of *nonoverlapping* Gaussians—the case near freezing— F_{id} [Eq. (2)] may be evaluated from the simple analytic expression

$$\beta F_{\text{id}}(x; \gamma_1, \gamma_2) / N = \frac{3}{2}(1-x) \ln \left[\frac{\gamma_1}{\pi} \right] + \frac{3}{2}x \ln \left[\frac{\gamma_2}{\pi} \right] - \frac{5}{2} + (1-x) \ln(1-x) + x \ln x + 3(1-x) \ln \lambda_1 + 3x \ln \lambda_2. \quad (9)$$

Next, F^{MWDA} is minimized with respect to γ_1 and γ_2 at fixed values of ρ_s and x (for a given choice of hard-sphere diameter ratio α). The existence of a local minimum implies that the solid is at least *mechanically* stable. Whether the solid is also *thermodynamically* stable is a matter to be decided by comparing its free energy with that of the fluid.

Finally, the freezing transition is located by identifying the thermodynamic state of fluid-solid coexistence, as characterized by equality of the temperature T , pressure P , and chemical potentials between the two phases. The relevant thermodynamic potential for this purpose is the Gibbs free energy per particle g , which is related to the

Helmholtz free energy per particle F/N by

$$g = F/N + P/\rho, \quad (10)$$

with P given by

$$P = \rho^2 \frac{\partial}{\partial \rho} (F/N). \quad (11)$$

At given values of T and P , equality of the chemical potentials is ensured by constructing a common tangent to the curves of g versus x for the two phases, the points of tangency occurring at the coexistence concentrations. For the solid, we obtain g from Eqs. (10) and (11), ap-

proximating F/N by the MWDA, as described above, and evaluating the derivative in Eq. (11) numerically. For the fluid, we adopt the analytic expression for g of Mansoori *et al.*,¹⁹ which is very accurate even at densities near freezing.¹⁸ By now varying T at fixed P , a temperature-concentration (T - x) phase diagram may be traced out. Figure 1 shows results at $P=1(k_B/\sigma_2^3)K$ for several values of the hard-sphere diameter ratio α , together with available simulation data.²⁰ The phase diagram is seen to evolve, with decreasing α , from a spindle

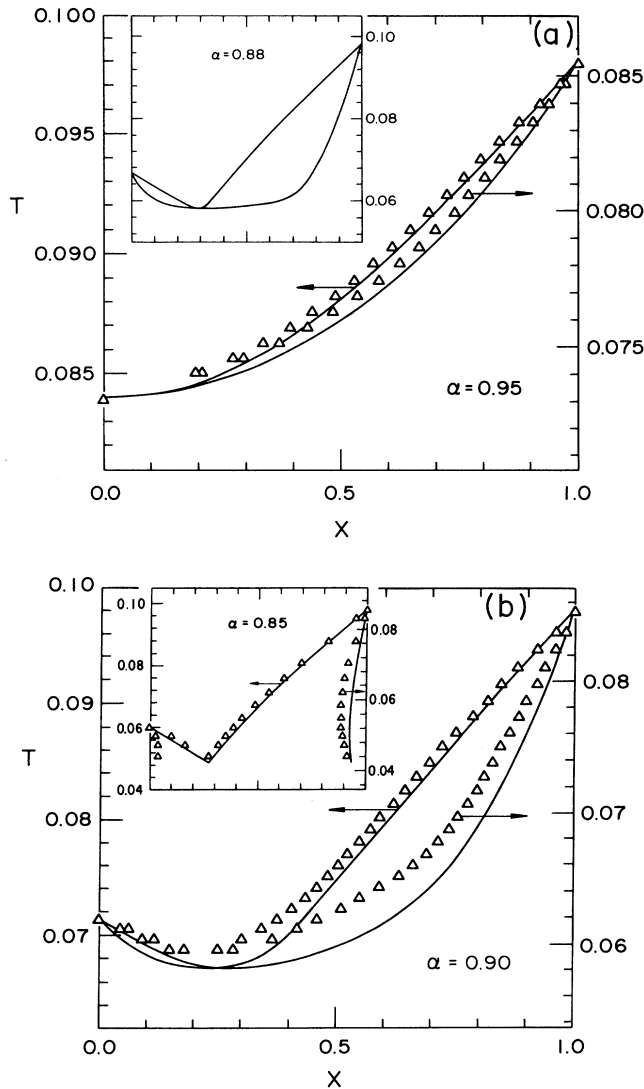


FIG. 1. Theoretical phase diagrams (solid curves) of temperature T (in units of K) vs concentration x (of the larger atoms) describing freezing of binary mixtures of hard spheres into a disordered-fcc crystal at pressure $P=1(k_B/\sigma_2^3)K$ at indicated values of the hard-sphere diameter ratio $\alpha=\sigma_1/\sigma_2$. The lower curves correspond to the solid phase, and the upper curves to the fluid phase. The open triangles represent corresponding simulation data from Refs. 20 and 21 plotted against normalized scales (see text for explanation).

type in the range $1 > \alpha > 0.94$ to an azeotropic type in the range $0.94 > \alpha > 0.87$ and finally to a eutectic type in the range $0.87 > \alpha$. After normalization to compensate for small discrepancies in the one-component limits⁶ (at $x=0$ and 1), theory and simulation are evidently in quite close quantitative agreement. Furthermore, the predictions of the theory for the onset of azeotropic behavior (at $\alpha=0.94$) and of eutectic behavior (at $\alpha=0.87$) are in excellent agreement with very recent simulation results.²¹

At given values of T , P , and x , the density of the solid ρ_s is next computed by numerically inverting the equation of state, i.e., $P=P(T, \rho_s, x)$ [Eq. (11)], and the fcc lattice constant is then immediately given by $a=(4/\rho_s)^{1/3}$. In this way, the lattice constant of the solid is obtained as a function of concentration x_s under fluid-solid coexistence conditions. Figure 2 shows resulting plots of a versus x_s corresponding to the phase diagrams in Fig. 1. The theoretical predictions are seen to adhere quite closely to a linear relationship at values of α sufficiently close to unity, but to deviate with increasing rapidity as α decreases, particularly near $x_s=1$. It may be observed that at $\alpha=0.85$, where the relationship is far from linear, the lattice constant can actually be double valued at a given concentration. By comparison with the phase diagram [inset to Fig. 1(b)], the two values are seen to correspond to solids that coexist at different temperatures with fluids of different concentrations.

In conclusion, the results of the (parameter-free) density-functional theory presented here demonstrate that, independent of other factors, a simple geometric difference in atomic sizes can play a significant role in determining the crystal structures—in particular, the

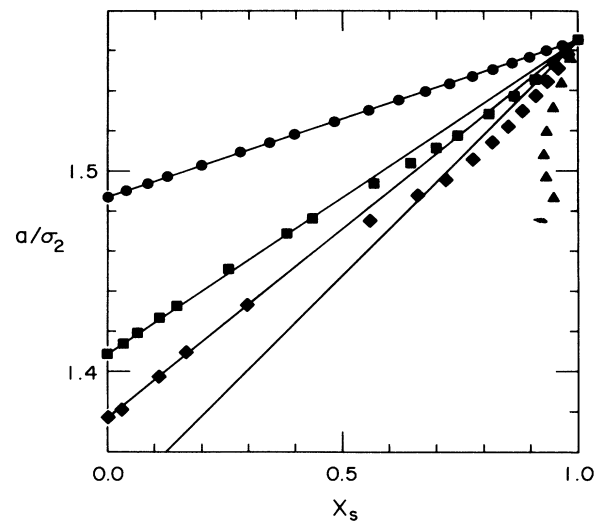


FIG. 2. Lattice constant a vs concentration x_s for a disordered-fcc hard-sphere crystal along the coexistence curves in Fig. 1. The symbols are predictions of the theory: circles ($\alpha=0.95$), squares ($\alpha=0.90$), diamonds ($\alpha=0.88$), triangles, ($\alpha=0.85$). Linear interpolations between $x_s=0$ and 1 illustrate that the relationship between a and x_s is very nearly linear for α sufficiently close to unity, but increasingly deviates from linearity as α decreases.

form of the lattice constant-concentration relationship—of binary alloys. They suggest, furthermore, that the linear relationship predicted by Vegard's law for alloys at constant temperature may also extend—for sufficiently small atomic-size disparities—to the fluid-solid coexistence curve, along which the temperature varies. It is important to emphasize, however, that in real alloys the form of the relationship may also be sensitive to other factors beyond the simple atomic-size factor considered here. Experimental determinations of lattice constants in alloys of varying concentrations at fluid-solid coexistence would clearly help to clarify this issue.

We are grateful to Dr. W. A. Curtin and to Professor N. D. Mermin for helpful discussions. This work was supported by National Science Foundation (NSF) Grant No. DMR-88-18558 through the Materials Science Center at Cornell University and NSF Grant No. DMR-8715590. One of us (A.R.D.) gratefully acknowledges partial support from the Natural Sciences and Engineering Research Council of Canada. The computations were performed using the Cornell National Supercomputer Facility, a resource of the Center for Theory and Simulation in Science and Engineering.

-
- ¹L. Vegard, *Z. Phys.* **5** 17 (1921); *Z. Kristallogr.* **67**, 239 (1928).
²C. S. Barrett, *Structure of Materials* (McGraw-Hill, New York, 1952).
³W. Hume-Rothery, R. E. Smallman, and C. W. Hayworth, *The Structure of Metals and Alloys* (The Metals and Metallurgy Trust, London, 1969).
⁴*Theory of Alloy Phase Formation*, edited by L. H. Bennett (The Metallurgical Society of AIME, New York, 1979).
⁵H. J. Axon and W. Hume-Rothery, *Proc. R. Soc. (London)*, Ser. A **A193**, 1 (1948).
⁶A. R. Denton and N. W. Ashcroft, *Phys. Rev. A* **42**, 7312 (1990).
⁷For recent reviews of the density-functional method and its applications to classical fluids, see D. W. Oxtoby, in *Liquids, Freezing, and the Glass Transition*, Les Houches session 51, edited by J. P. Hansen, D. Levesque, and J. Zinn-Justin (Elsevier, New York, 1990); M. Baus, *J. Phys. Condens. Matter* **2**, 2111 (1990); R. Evans, in *Liquids at Interfaces*, Les Houches session 48, edited by J. Charvolin, J. F. Joanny, and J. Zinn-Justin (Elsevier, New York, 1989); M. Baus, *J. Stat. Phys.* **48**, 1129 (1987); A. D. J. Haymet, *Prog. Solid State Chem.* **17**, 1 (1986).
⁸J. L. Barrat, M. Baus, and J. P. Hansen, *Phys. Rev. Lett.* **56**, 1063 (1986); *J. Phys. C* **20**, 1413 (1987).
⁹R. Evans, *Adv. Phys.* **28**, 143 (1979).
¹⁰A. R. Denton and N. W. Ashcroft, *Phys. Rev. A* **39**, 4701 (1989). The MWDA is a computationally simpler modification of the weighted-density approximation of W. A. Curtin and N. W. Ashcroft, *Phys. Rev. A* **32**, 2909 (1985); *Phys. Rev. Lett.* **56**, 2775 (1986). See also P. Tarazona, *Mol. Phys.* **52**, 81 (1984); *Phys. Rev. A* **31**, 2672 (1985).
¹¹N. W. Ashcroft and D. C. Langreth, *Phys. Rev.* **156**, 685 (1967); **166**, 934(E) (1967).
¹²D. A. Young and B. J. Alder, *J. Chem. Phys.* **60**, 1254 (1974).
¹³B. B. Laird, J. D. McCoy, and A. D. J. Haymet, *J. Chem. Phys.* **87**, 5449 (1987).
¹⁴J. L. Colot, M. Baus, and H. Xu, *Mol. Phys.* **57**, 809 (1986).
¹⁵W. A. Curtin and K. Runge, *Phys. Rev. A* **35**, 4755 (1987).
¹⁶In computing the weighted densities from Eq. (8), we have included 100–150 reciprocal-lattice-vector shells (a shell comprising all vectors of the same magnitude) to ensure convergence of the sum.
¹⁷J. L. Lebowitz, *Phys. Rev.* **133**, A895 (1964). The Fourier transforms of $c_{ij}^{(2)}(r)$ have been given explicitly by Ashcroft and Langreth. See Ref. 11.
¹⁸G. Jackson, J. S. Rowlinson, and F. van Swol, *J. Phys. Chem.* **91**, 4907 (1987); P. H. Fries and J. P. Hansen, *Mol. Phys.* **48**, 891 (1983); B. J. Alder, *J. Chem. Phys.* **40**, 2724 (1964).
¹⁹G. A. Mansoori, N. F. Carnahan, K. E. Starling, and T. W. Leland, Jr., *J. Chem. Phys.* **54**, 1523 (1971). Note that in applying the MWDA, we choose the PY approximation for the uniform-state excess free energy over the more accurate expression of Mansoori *et al.* This is consistent with our use of the PY approximations for the two-particle DCF's, for which there exist, to our knowledge, no alternatives consistent with the excess free energy of Mansoori *et al.*
²⁰W. G. T. Kranendonk and D. Frenkel, *J. Phys. Condens. Matter* **1**, 7735 (1989).
²¹W. G. T. Kranendonk, Ph.D. thesis, University of Utrecht, 1990; W. G. T. Kranendonk and D. Frenkel, *Mol. Phys.* (to be published).